

WALDEMAR MINKINA, SŁAWOMIR GRYŚ

Czestochowa University of Technology
Institute of the Electronics and Control Systems
Poland, e-mail: minkina@el.pcz.czyst.pl

DYNAMICS OF CONTACT THERMOMETRIC SENSORS WITH ELECTRIC OUTPUT AND METHODS OF ITS IMPROVEMENT

The paper deals with selected aspects of modelling dynamic properties of contact thermometric sensors and reducing the dynamic error occurring in measurement of time-variable temperature as well as in measurement of constant temperature while the sensor output is settling. Due to volume limitations the paper is only an outline and presents some problems superficially. An attempt to present a wider study on the subject with rich bibliography is presented in the authors' monograph [1].

Keywords: thermometer sensor, dynamic properties, correction algorithms

1. INTRODUCTION

Neglecting static and dynamic parameters of the sensors can lead to erroneous interpretation of measurement results. In many situations it results in degradation of the process control performance or possible damage of the production line components due to incorrect action of the control system actuators. Good examples of industry applications, where rapid growth of the temperature can result in possible disaster, are: nuclear power plants, chemical industry, and aviation or machine industry. Static error correction does not involve serious problems. The dynamic properties of e.g. a thermometric sensor are connected with its thermal inertia and thermal resistance between the medium and the sensor.

2. MODELS OF DYNAMIC PROPERTIES

Expertise on dynamic properties of a sensor makes the determination of the dynamic component of the measurement error possible. In the case of a thermometric sensor it is also a key factor that makes possible appropriate choice of:

- correct model of the dynamics,
- correction system and its parameters while measuring variable temperature,
- sample time for discrete-time models in computerised measuring systems.

2.1. Linear models

Most contact thermometric sensors can be considered as a homogeneous cylinder of mass m , thermal conductivity λ , specific heat c_p , heat transfer surface F and heat transfer coefficient α . For a sufficiently great value of λ and sufficiently small cylinder diameter such a sensor can be considered, for small increments of the temperature, as a linear element described by a first order differential equation with constant parameters:

$$N_T \frac{dT_T}{d\tau} + T_T = T, \quad (1)$$

where:

$$N_T = \frac{mc_p}{\alpha F} \quad (2)$$

and T - temperature (sensor input signal), T_T - measured temperature (sensor output signal).

Table 1. Transfer function models of sensors' dynamics.

Transfer function	Response to temperature step from T_p to T_m .	Eq. No.
$G_T(s) = \frac{1}{(N_T s + 1)}$	$T_T(\tau) = T_p + (T_m - T_p) \cdot \left[1 - \exp\left(-\frac{\tau}{N_T}\right) \right]$	3.1
$G_T(s) = \frac{1}{(N_{T1}s+1)(N_{T2}s+1)}$	$T_T(\tau) = T_p + (T_m - T_p) \cdot \left[1 - \frac{N_{T1}}{N_{T1} - N_{T2}} \exp\left(-\frac{\tau}{N_{T1}}\right) + \frac{N_{T2}}{N_{T1} - N_{T2}} \exp\left(-\frac{\tau}{N_{T2}}\right) \right]$ $N_{T1} \neq N_{T2}$	3.2
$G_T(s) = \frac{N_{T3}s+1}{(N_{T1}s+1)(N_{T2}s+1)}$	$T_T(\tau) = T_p + (T_m - T_p) \cdot \left[1 - \frac{N_{T1} - N_{T3}}{N_{T1} - N_{T2}} \exp\left(-\frac{\tau}{N_{T1}}\right) + \frac{N_{T2} - N_{T3}}{N_{T1} - N_{T2}} \exp\left(-\frac{\tau}{N_{T2}}\right) \right]$ $N_{T1} \neq N_{T2} \neq N_{T3}$	3.3
$G_T(s) = \frac{e^{-sN_{T3}}}{(N_{T1}s+1)(N_{T2}s+1)}$	$T_T(\tau) = T_p + (T_m - T_p) \cdot \left[1 - \frac{N_{T1}}{N_{T1} - N_{T2}} \exp\left(-\frac{\tau - N_{T3}}{N_{T1}}\right) + \frac{N_{T2}}{N_{T1} - N_{T2}} \exp\left(-\frac{\tau - N_{T3}}{N_{T2}}\right) \right]$ $N_{T1} \neq N_{T2} \quad \tau \geq N_{T3}$	3.4
$G_T(s) = \frac{1}{\cosh \sqrt{N_T} s}$	$T_T(\tau) = T_p + (T_m - T_p) \cdot \left\{ 1 - \frac{4}{\pi} \sum_{n=0}^{\infty} \frac{(-1)^n}{2n+1} \exp\left[-\frac{\pi^2}{4N_T} (2n+1)^2 \tau\right] \right\}$	3.5
$G_T(s) = \frac{1}{\exp \sqrt{N_T} s}$	$T_T(\tau) = T_p + (T_m - T_p) \cdot \left[1 - \frac{2}{\sqrt{\pi}} \sum_{n=0}^{\infty} (-1)^n \frac{\left(\frac{1}{2} \sqrt{\frac{N_T}{\tau}}\right)^{2n+1}}{n!(2n+1)} \right] \quad \tau > 0$	3.6
$G_T(s) = \frac{1}{(N_T s + 1)^r}$	$T_T(\tau) = T_p + (T_m - T_p) \cdot \left[1 - \exp\left(-\frac{\tau}{N_T}\right) \cdot \sum_{n=0}^{r-1} \frac{1}{n!} \cdot \left(\frac{\tau}{N_T}\right)^n \right] \quad r - \text{natural}$	3.7
	$T_T(\tau) = T_p + (T_m - T_p) \cdot \frac{1}{\Gamma(r)} \left[\sum_{n=0}^{\infty} (-1)^n \frac{1}{n!(n+r)} \cdot \left(\frac{\tau}{N_T}\right)^{n+r} \right] \quad r - \text{rational}$ $\Gamma - \text{Euler gamma function}$	3.8

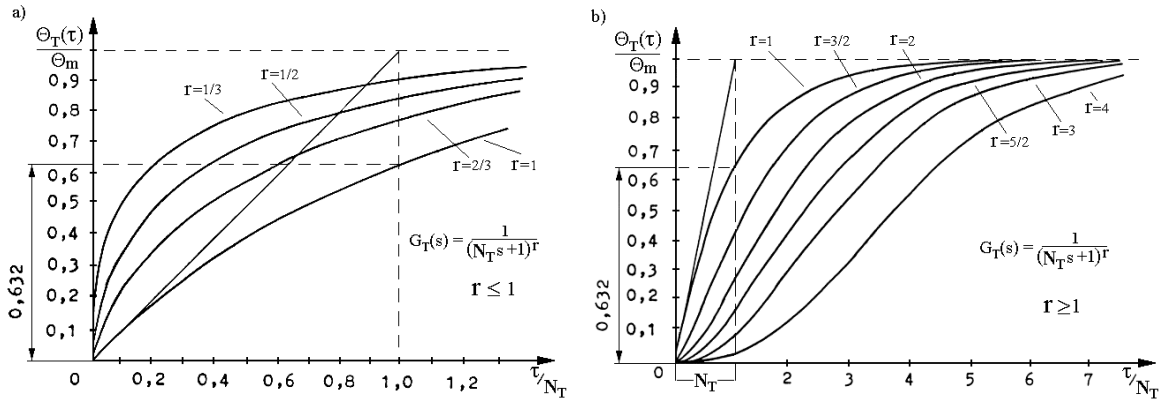


Fig. 1. Step response of sensor described by transfer function (3.8).

For a step input signal the time constant N_T is equal to the time after which the sensor output reaches 0.632 of the input step value. The concept of temperature increment: $\Theta_T(\tau) = T_T(\tau) - T_p$ and $\Theta(\tau) = T(\tau) - T_p$ is used to obtain zero initial conditions, which enables the sensor's dynamics to be described in the frequency domain using the transfer function. Typical transfer function models are collected in Table 1 on the basis of [1-4]. The sensor construction and conditions of the heat transfer between the sensor and the medium the temperature of which is measured, are the basis of decision which specific transfer function should be chosen. The last of the models, described by (3.8), has particular properties. Choosing an appropriate value of the parameter r it is possible to obtain step responses similar to responses of the remaining models (except the model with the transport delay (3.4)). The step responses of model (3.8) for different values of r are shown in Fig.1 [5]. In practice, it is not recommended to use models of order greater than 4 because usually it does not improve the accuracy of approximation of real sensor dynamic parameters and involves amplification of noise when correction systems or algorithms are applied. The step responses of real sensors, according to their construction, are presented in Fig.2.

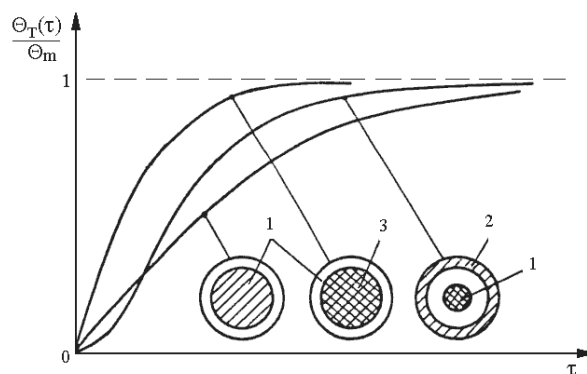


Fig. 2. Step responses of real sensors, where: 1 – sensitive part of the sensor, 2 - shield, 3 – insulating shell.

2.2. Nonlinear models

Application of linear models is reasonable when the simplifications do not cause significant discrepancy between responses of the real sensor and its model. For greater increments of temperature which most often occur in practice, the thermal parameters of materials the thermometer is built of, change with temperature. Moreover, the heat transfer between the medium and the sensor is mainly radiative. It imposes the application of nonlinear models that takes into consideration changes of the “time constant” dependent on the measured temperature T_m and the sensor instant temperature T_T . Existence of this changeability gives reason to introduce the concept of *dynamic parameter* instead of *time constant*:

$$N_T(T_T, T_m) = \frac{mc_p(T_T, T_m)}{F\alpha(T_T, T_m)}, \quad (4)$$

which means that, after substituting (4) into (1), the dynamic properties of the thermometer are described by a nonlinear differential equation.

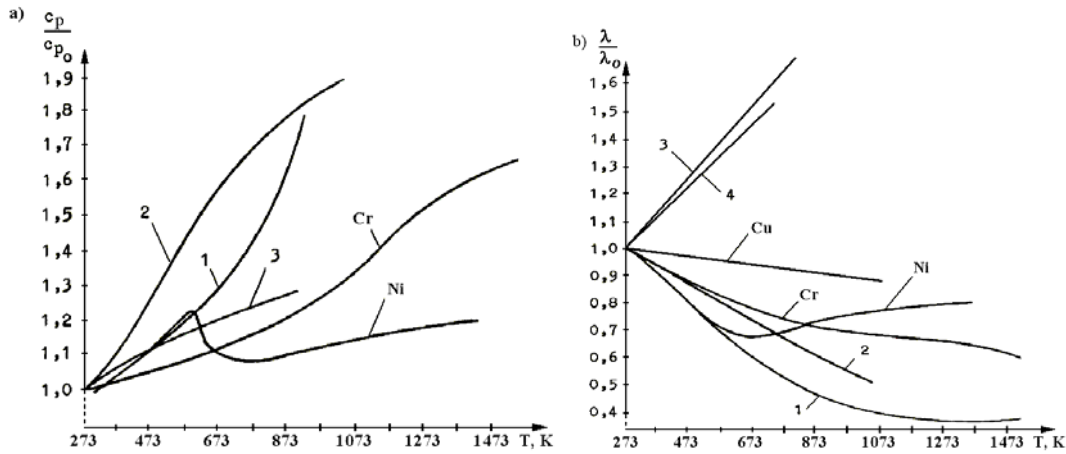


Fig. 3. Specific heat c_p (a) and heat transfer coefficient λ (b) versus temperature for different metals used to build thermocouples: 1 - iron, 2 - low-carbon steel, 3 - stainless heat resisting steel: 12X18H10T, 4 - alloy: 90%Ni, 10%Cr.

The dependence of the specific heat c_p and the heat transfer coefficient α on temperature in the above equation is difficult to define because these quantities depend on many factors, like material and construction properties or operating conditions of the thermometer. The changes of the specific heat c_p with temperature T for selected materials that are used to build thermometers are shown in Fig.3a. The values of c_p are given with reference to c_{p0} , i.e. the specific heat at 273K.

The second quantity responsible for dynamic nonlinearity of the sensor is thermal conductivity λ (Fig.3b). The dependence of λ on the temperature should be taken into account in one- or two-dimensional models of heat transfer at the cross-section as well as along the sensor.

The heat transfer coefficient α is also strongly temperature-dependent. We can distinguish its two components:

$$\alpha(T_T, T_m) = \alpha_k(T_T, T_m) + \alpha_r(T_T, T_m), \quad (5)$$

where: α_k - convective heat transfer coefficient, α_r - radiative heat transfer coefficient, W/(m²K). The dependence of α_k on the temperature and the thermometer diameter d is described by:

$$\alpha_k(T_T, T_m) = A_2(T') \left(\frac{T_m - T_T}{d} \right)^{1/4}. \quad (6)$$

The parameter A_2 , W/(m^{7/4}K^{5/4}) is a function of mean temperature $T' = (T_m + T_T)/2$ and this relationship is strongly nonlinear. The value of A_2 depends on the medium, its velocity and pressure. Equation (6) follows from generalizations related to investigations on so called dimensionless equations. The second component in (5), i.e. α_r , is strictly defined by the analytic relationship:

$$\alpha_r(T_T, T_m) = \sigma_o \varepsilon \frac{T_m^4 - T_T^4}{T_m - T_T}, \quad (7)$$

where: ε - emissivity of the sensor material, $\sigma_o = 5.67 \cdot 10^{-8}$ W/(m²K⁴) - Stefan-Boltzmann constant of blackbody radiation.

For purely radiative heat transfer the thermometer's nonlinear dynamic model can be derived from the following heat balance:

$$mc_p \frac{dT_T}{d\tau} = \sigma_o \varepsilon F (T_m^4 - T_T^4). \quad (8)$$

The above equation can be transformed into:

$$N_T(T_T, T_m) \frac{dT_T}{d\tau} + T_T = T_m. \quad (9)$$

In this case the dynamic parameter is defined as:

$$N_T(T_T, T_m) = \frac{c_p \rho d}{4\sigma_o \varepsilon} \cdot \frac{1 - \frac{T_T(\tau)}{T_m}}{T_m^3 \left\{ 1 - \left[\frac{T_T(\tau)}{T_m} \right]^4 \right\}}, \quad (10)$$

where its initial value N_{T_p} - at temperature T_p , and final value N_{T_m} - at temperature T_m , are defined as:

$$N_{T_p} = \frac{c_{p_o} \rho d}{4\sigma_o \varepsilon T_m^3}, \quad N_{T_m} = \frac{c_{p_m} \rho d}{16\sigma_o \varepsilon T_m^3}, \quad (11)$$

where c_{p_o} and c_{p_m} are values of c_p at temperature T_p and T_m respectively and ρ is the density, kg/m³.

In practice, taking into consideration the temperature dependence of the specific heat, the material parameters (density, emissivity) and the sensor dimensions (radius) is very burdensome. Therefore, it is convenient to use substitute nonlinear models derived for specific constant conditions of the heat transfer. One solution is to assume that changes of the dynamic parameter can be described by a polynomial (over some range of operating temperatures) of the current temperature, e.g.:

$$N_T(t_T) = N_{Tp} + bt_T + at_T^2 \quad (12)$$

or

$$N_T(t_T) = N_{Tp} \exp(at_T), \quad (13)$$

where: N_{Tp} - initial value of the dynamic parameter at initial temperature T_p , s; b - first order coefficient of nonlinearity, s/°C; a - second order coefficient of nonlinearity, s/(°C)². Step responses of different nonlinear models [6], under assumption $t_p = 0^\circ\text{C}$, can be compared in Fig. 4.

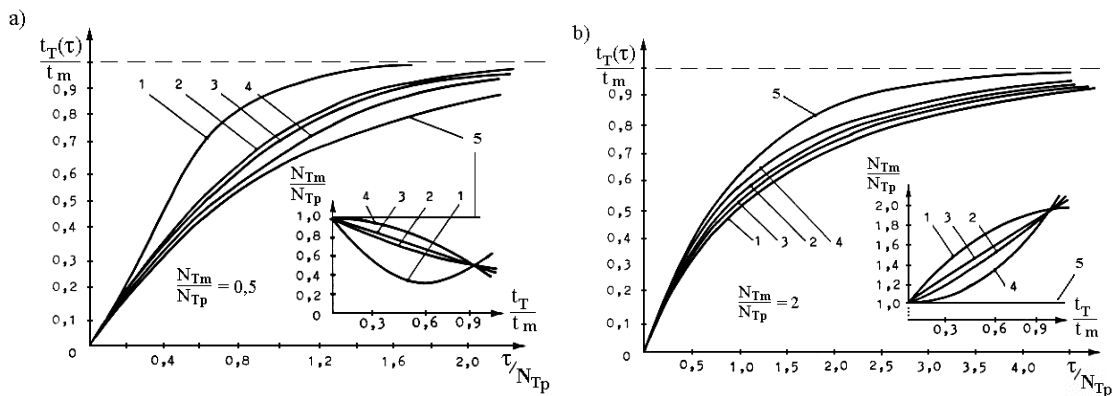


Fig. 4. Step responses for different values of ratio N_{Tm}/N_{Tp} obtained for: (a) 1 - Eq. (12) for $a>0$ and $b<0$, 2 - Eq. (13) for $a<0$, 3 - Eq. (12) for $a=0$ and $b<0$, 4 - Eq. (12) for $a<0$ and $b=0$, 5 - Eq. (3.1), (b) 1 - Eq. (12) for $a<0$ and $b>0$, 2 - Eq. (13) for $a>0$, 3 - Eq. (12) for $a=0$ and $b>0$, 4 - Eq. (12) for $a>0$, 5 - Eq. (3.1).

3. IMPROVEMENT METHODS OF DYNAMIC PROPERTIES

Reduction of the dynamic error can be obtained by:

- elimination of air gaps,
- reduction of sensor dimensions,
- using materials with better heat conductivity for sensor shells,
- using heat-conductive paste (in measurements of surface temperature),
- increasing contact pressure and surface.

However, the sensor construction and positioning are frequently determined by chemical aggressiveness of the environment, pressure, vibrations and shocks, range of measured temperatures or measurement method. Then, if the dynamic properties of the sensor are still unsatisfactory, significant improvement can be achieved by applying one of the methods

described in the literature. A classification of methods used to “improve” the dynamic properties or partly compensate their influence on the temperature measurement error is presented in Fig.5.

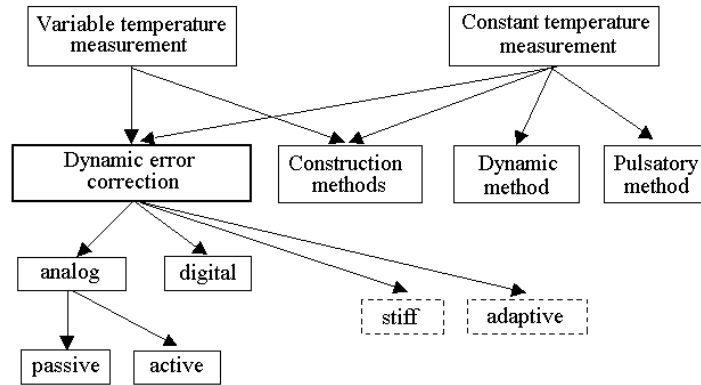


Fig. 5. Classification of methods used to improve dynamic properties of thermometric sensors.

3.1. Construction methods

In the case of thermocouples, better dynamic properties can be achieved using the construction with three measuring junctions, the so-called multijunction effect, as shown in Fig.6a [7]. A metal cylinder connected to the middle junction deteriorates its dynamic properties. The formula for the thermoelectric value of such a sensor design is derived in [1]. Consequently we obtain the following formula for the step response [1]:

$$T_T(\tau) = T_p + (T_m - T_p) \left[1 - \exp\left(-\frac{\tau}{N_{T1}}\right) + \exp\left(-\frac{\tau}{N_{T2}}\right) - \exp\left(-\frac{\tau}{N_{T3}}\right) \right], \quad (14)$$

where: N_{T1} - time constant of junction 1 (Fig. 6a), N_{T2} - time constant of junction 2, and so on.

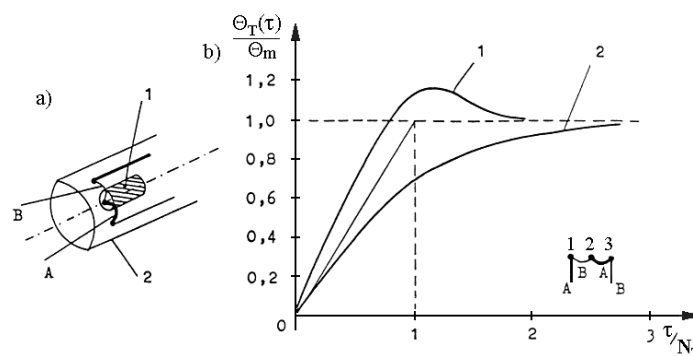


Fig. 6. a) Thermocouple with additional metal cylinder: 1- metal cylinder, 2- shield, A, B - thermocouple wires, b) Step responses for different N_{T2}/N_T .

The step responses of model (14) for the following conditions: $N_{T1} = N_{T3} = N_T$ and $N_{T2}/N_T = < 1, 1.25, 1.5, 1.75, 2 >$, are shown in Fig.6b. One can see that if $1 < N_{T2}/N_T < 1.5$, the dynamic

processing of the thermocouple is clearly better despite the presence of the cylinder which increases the time constant N_{T2} of the middle junction even by 50%.

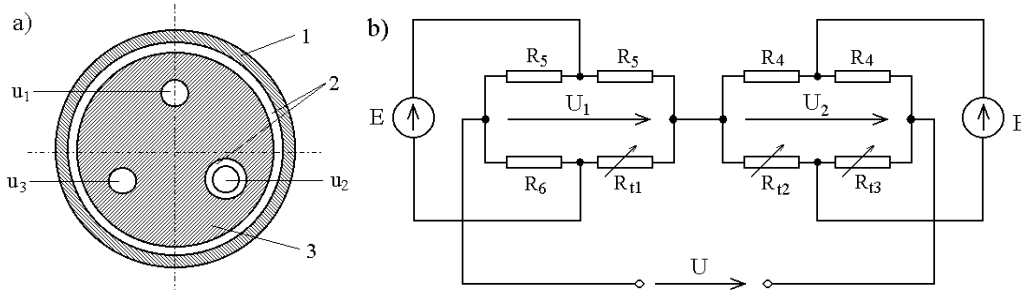


Fig. 7. a) Cross-section of three winding thermometer resistor, b) Two-bridge circuit.

The idea of three sensors with reference to thermometric resistors is presented in Fig.7 [8]. In the two-bridge circuit in Fig.7b the three sensors from Fig.7a are represented by three resistances: resistance R_{t1} represents winding u_1 , resistance R_{t2} represents winding u_2 and resistance R_{t3} represents winding u_3 . The derivation of the formula for the voltage U of the bridge is given in [1]. Practical realization of this method consists in constructing a resistor with three windings, whose second winding (2) should have worse dynamics than the remaining two (1 and 3). The worse dynamics can be achieved by increasing the hole (air gap) in which it is mounted. The formula for the step response is identical to the one obtained for the three-junction thermocouple (Eq. (14)).

3.2. Dynamic method

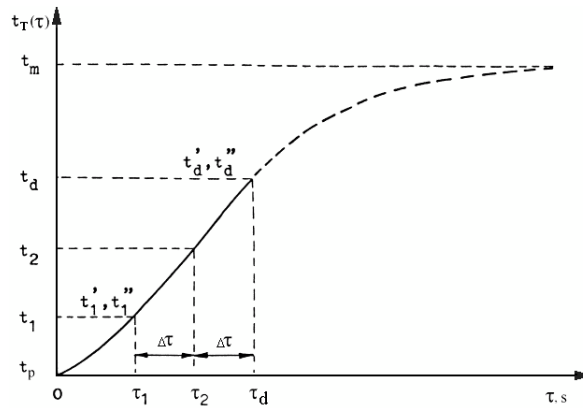


Fig. 8. Idea of high temperature measurement using dynamic method.

In the dynamic method the sensor is quickly put into the medium whose temperature is measured and its response is recorded. If the steady-state temperature t_m exceeds the temperature t_d permissible for the sensor, it is removed back to the original environment when its temperature achieves t_d . The measurement time is restricted to minimum, so only a part of the step response can be recorded. This fact is illustrated in Fig.8. Table 2 includes formulas that make it possible to determine the true steady-state temperature assuming that $t_m \gg t_p$ and that the sensor's

dynamics is described by a first-order linear model (3.1). Therefore, the initial part of the recorded step response, i.e. until τ_1 , is discarded. The method defined by Eq. (15) presented in Table 2 is sensitive to random errors and may lead to significant errors in determining (predicting) the temperature t_m because it uses only few samples (maximum 4) of the sensor output signal. Determining the steady-state temperature on the basis of a greater number of samples can be realized using the least squares method as the identification method. This solution can be applied for linear models (3) as well as for substitute nonlinear models defined e.g. by (12) or (13). Other solutions of the prediction problem are also considered in the literature. One of them is based on application of artificial feedforward neural network [1]. The advantage of such attitude is that it does not require assuming analytical model of the sensor's dynamic properties. Moreover, the computations at the prediction stage are relatively not complex in contrast to the training stage. The drawback of this method is necessity of re-training the network when the sensor type or the heat transfer conditions.

Table 2. Different methods to determine the steady-state temperature.

Input quantities	Formula for t_m	Eq. No.
t_d $t_d' = \frac{dt}{d\tau} \Big _{(\tau_d, t_d)}$ $t_d'' = \frac{d^2t}{d\tau^2} \Big _{(\tau_d, t_d)}$	$t_m = t_d - \frac{(t_d')^2}{t_d''}$	15.1
$t_1; t_d;$ $t_1' = \frac{dt}{d\tau} \Big _{(\tau_1, t_1)}; t_d' = \frac{dt}{d\tau} \Big _{(\tau_d, t_d)}$	$t_m = \frac{t_d t_1' - t_1 t_d'}{t_1 - t_d}$	15.2
$t_1; t_2; t_d; \Delta\tau = const$ $\Delta t_1 = t_d - t_2; \Delta t_2 = t_2 - t_1$	$t_m = \frac{\Delta t_1^2}{\Delta t_2 - \Delta t_1} + t_d$	15.3
$t_1; t_2; t_d; \Delta\tau = const$ $t_1 = t_m \cdot \left[1 - \exp\left(-\frac{\tau_1}{N}\right) \right]$ $t_2 = t_m \cdot \left[1 - \exp\left(-\frac{\tau_1 + \Delta\tau}{N}\right) \right]$ $t_d = t_m \cdot \left[1 - \exp\left(-\frac{\tau_1 + 2\Delta\tau}{N}\right) \right]$	$t_m = \frac{t_2^2 - t_1 t_d}{2t_2 - t_d - t_1}$	15.4

$t_1; t_2; t_3; t_d; \Delta\tau = const$ $t_1 = t_m \cdot \left[1 - \exp\left(-\frac{\tau_1}{N}\right) \right]$ $t_2 = t_m \cdot \left[1 - \exp\left(-\frac{\tau_1 + \Delta\tau}{N}\right) \right]$ $t_3 = t_m \cdot \left[1 - \exp\left(-\frac{\tau_1 + 2\Delta\tau}{N}\right) \right]$ $t_d = t_m \cdot \left[1 - \exp\left(-\frac{\tau_1 + 3\Delta\tau}{N}\right) \right]$	$t_m = \frac{t_2 t_3 - t_1 t_d}{t_3 + t_2 - t_d - t_1}$	15.5
---	---	------

3.3. Dynamic error correction

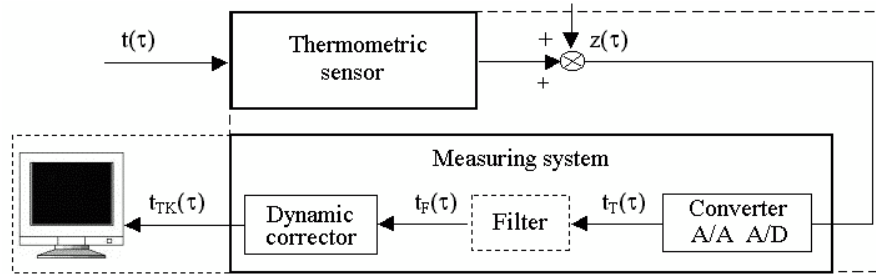


Fig. 9. Flow of the signal in the measurement path.

The correction is carried out in the measuring chain, typical for measurements of physical quantities (Fig.9). The sensor output signal is usually an electric quantity, current or voltage, whose value depends on the measured temperature. An additive signal $z(\tau)$ represents the influence of external electromagnetic fields and network disturbances. The task of the A/A converter is usually amplification of the signal, static error correction or, in the case of thermocouples, correction of the reference junction temperature. The lowpass filter suppresses transmission of disturbances to the input of the dynamic corrector. The correction and filtration can be realized entirely as analog or digital. However, the application range of analog correctors is limited to measurements of small temperature increments in constant heat transfer conditions. The description of analog correctors systems is presented e.g. in [1]. Passive correctors are built as R, L, C circuits while the active ones contain additional operational amplifiers to compensate for the attenuation of the measured signal. Digital correction offers much wider opportunities. Therefore modern automatics systems are realized mostly as hybrid systems. The analog part of the system is the sensor along with conditioning circuits that match the signal to the A/C converter input. Further processing of the signal is digital, and the correction algorithm is implemented in software or hardware, e.g. by using an external digital filter (Fig.10). Such a filter is described by the corrector transfer function in the z-operator domain:

$$G_K(z) = \frac{a_0 + a_1 z^{-1} + a_2 z^{-2} + \dots + a_m z^{-m}}{1 + b_1 z^{-1} + b_2 z^{-2} + \dots + b_n z^{-n}}. \quad (16)$$

If we assume $m=1$, $n=0$ in (16) and choose “matched pole-zero” as the discretization method, the coefficients of the corrector processing the output signal of the sensor modelled by transfer function (3.1) are defined as follows:

$$a_0 = \frac{1}{1 - \exp\left(\frac{-h}{N_K}\right)}, \quad a_1 = -a_0 \exp\left(\frac{-h}{N_K}\right). \quad (17)$$

On the basis of the analysis presented in [1], it is possible to give the following rule of selection of the discretization step h (which is the inverse of the sampling frequency):

$$h \leq \frac{\pi}{100} N_T \approx 0,03 N_T. \quad (18)$$

Satisfying condition (18) guarantees absence of aliasing on the one hand and an acceptable level of disturbances and noise transmitted to the corrector input on the other hand. In practice, the value of h depends on the hardware capabilities or specification of the measurement system. Regardless of the applied hardware - analog or digital, the corrector parameters are adequate only for conditions in which the identification of the sensor’s dynamics was performed.

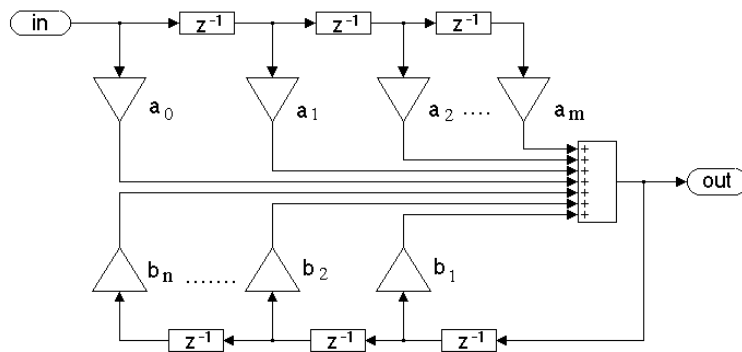


Fig. 10. Digital finite impulse response filter

The methods of determining the parameters of linear models of the sensor’s dynamics are commonly known [2-4,9]. The parameters of nonlinear (linear as well) models defined e.g. by (12), can be determined using the method of the least sum of squares. The algorithm is presented further in the vector notation and iterative version, convenient for computer implementation [1].

Let the minimized function be defined as:

$$V(\mathbf{x}) = \frac{1}{2} \sum_{i=1}^M F_i^2(\mathbf{x}) = \frac{1}{2} \mathbf{F}^T(\mathbf{x}) \mathbf{F}(\mathbf{x}), \quad (19)$$

where: $\mathbf{x} = [x_1 \ x_2 \ \dots \ x_K]^T$ - vector of K unknown parameters of dynamics model, K - number of parameters, M - number of recorded samples.

Such a form of the function $V(\mathbf{x})$ ensures the existence of a unique minimum at which the gradient is zero. The vector $\mathbf{F}(\mathbf{x})$ includes differences between the model response and the samples measured at consecutive time instants τ_i :

$$\mathbf{F}(\mathbf{x}) = \begin{bmatrix} F_1(\mathbf{x}) \\ F_2(\mathbf{x}) \\ \vdots \\ F_M(\mathbf{x}) \end{bmatrix}, \quad (20)$$

where:

$$F_i(\mathbf{x}) = t_m - N_T(t_T(\tau_i)) \frac{dt_T(\tau_i)}{d\tau_i} - t_T(\tau_i), \quad i = 1, \dots, M. \quad (21)$$

The expression $N_T(t_T)$ in (21) describes variations of the dynamic parameter of the sensor, defined e.g. by (12). Depending on the complexity of the model, the vector \mathbf{x} has one of the following forms:

$$N_{T_p} \Rightarrow \mathbf{x} = [N_{T_p}]^T \quad K=1 \quad (22a)$$

$$N_T(t_T) = N_{T_p} + bt_T \Rightarrow \mathbf{x} = [N_{T_p} \quad b]^T \Rightarrow K=2 \quad (22b)$$

$$N_{T_p} + bt_T + at_T^2 \Rightarrow \mathbf{x} = [N_{T_p} \quad b \quad a]^T \quad K=3 \quad (22c)$$

The *gradient* is defined as a vector of partial derivatives (23), whereas the *Jacobian* matrix is defined by (24):

$$\nabla V(\mathbf{x}) = \begin{bmatrix} \frac{\partial V(\mathbf{x})}{\partial x_1} \\ \frac{\partial V(\mathbf{x})}{\partial x_2} \\ \vdots \\ \frac{\partial V(\mathbf{x})}{\partial x_K} \end{bmatrix}, \quad (23)$$

$$\dim \nabla V(\mathbf{x}) = K \times 1$$

$$\mathbf{J}(\mathbf{x}) = \begin{bmatrix} \frac{\partial \mathbf{F}_1(\mathbf{x})}{\partial x_1} & \dots & \frac{\partial \mathbf{F}_1(\mathbf{x})}{\partial x_K} \\ \vdots & \ddots & \vdots \\ \frac{\partial \mathbf{F}_M(\mathbf{x})}{\partial x_1} & \dots & \frac{\partial \mathbf{F}_M(\mathbf{x})}{\partial x_K} \end{bmatrix}. \quad (24)$$

$$\dim \mathbf{J}(\mathbf{x}) = M \times K$$

For the matrices defined in this way, we can write:

$$\nabla V(\mathbf{x}) = \mathbf{J}^T(\mathbf{x})\mathbf{F}(\mathbf{x}), \quad (25)$$

$$\mathbf{H}(\mathbf{x}) = \mathbf{J}^T(\mathbf{x})\mathbf{J}(\mathbf{x}) + \mathbf{Q}(\mathbf{x}), \quad (26)$$

where:

$$\mathbf{Q}(\mathbf{x}) = \sum_{i=1}^M \mathbf{F}_i(\mathbf{x})\mathbf{H}_i(\mathbf{x}). \quad (27)$$

The matrix $\mathbf{H}_i(\mathbf{x})$ is the *Hessian* for the i -th time instant defined as:

$$\mathbf{H}_i(\mathbf{x}) = \begin{bmatrix} \frac{\partial^2 \mathbf{F}_i(\mathbf{x})}{\partial x_1 x_1} & \dots & \frac{\partial^2 \mathbf{F}_i(\mathbf{x})}{\partial x_1 x_K} \\ \vdots & \ddots & \vdots \\ \frac{\partial^2 \mathbf{F}_i(\mathbf{x})}{\partial x_K x_1} & \dots & \frac{\partial^2 \mathbf{F}_i(\mathbf{x})}{\partial x_K x_K} \end{bmatrix}. \quad (28)$$

Assuming iterative updating elements of \mathbf{x} using the Newton method, we should compute the Hessian inverse in each iteration j because

$$\mathbf{x}_{j+1} = \mathbf{x}_j - \mathbf{H}^{-1}(\mathbf{x}_j)\nabla V(\mathbf{x}_j). \quad (29)$$

It is a time consuming and numerically complex task because of the term $\mathbf{Q}(\mathbf{x})$ appearing in (26). Practical applications are designed to work with approximate computation of the Hessian. By discarding $\mathbf{Q}(\mathbf{x})$ we obtain the Gauss-Newton algorithm which is simple in realization but its drawback is weak convergence, because the discarded term carries significant information. In the Levenberg-Marquardt algorithm $\mathbf{Q}(\mathbf{x})$ is replaced by a normalizing term which is adaptively updated while the algorithm approaches the optimum solution. The parameter vector is updated as follows:

$$\mathbf{x}_{j+1} = \mathbf{x}_j - [\mathbf{J}^T(\mathbf{x}_j)\mathbf{J}(\mathbf{x}_j) + \gamma_j \mathbf{I}]^{-1} \mathbf{J}^T(\mathbf{x}_j)\mathbf{F}(\mathbf{x}_j). \quad (30)$$

For $\gamma=0$ we get the Gauss-Newton method. When γ tends to infinity, the elements of the Hessian tend asymptotically to constant values, which is equivalent to the steepest descent method.

3.4. Adaptive correction using the two-sensor method

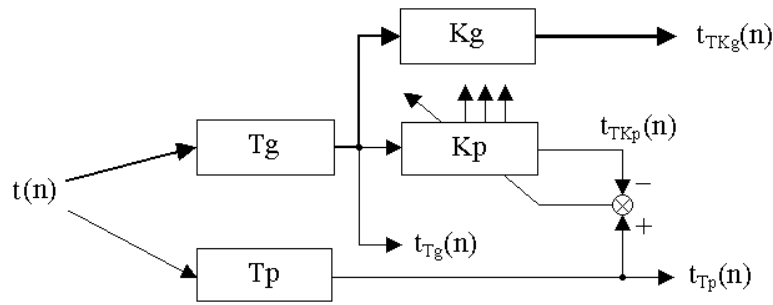


Fig. 11. Adaptive correction using two sensors with different dynamic properties.

Any change of the heat transfer conditions, caused e.g. by a change of the medium velocity or change of the measured temperature range, results in the necessity of repeating the identification of the sensor model. This is called adaptive correction because the algorithm reacts to changes of the operating conditions. Lack of information from the sensor input makes it impossible to conduct any classical parameter identification of the sensor in real conditions. Assuming arbitrary changes of the temperature with time, the correction problem can be solved e.g. using a system with two or more sensors whose dynamic properties are different [10-14].

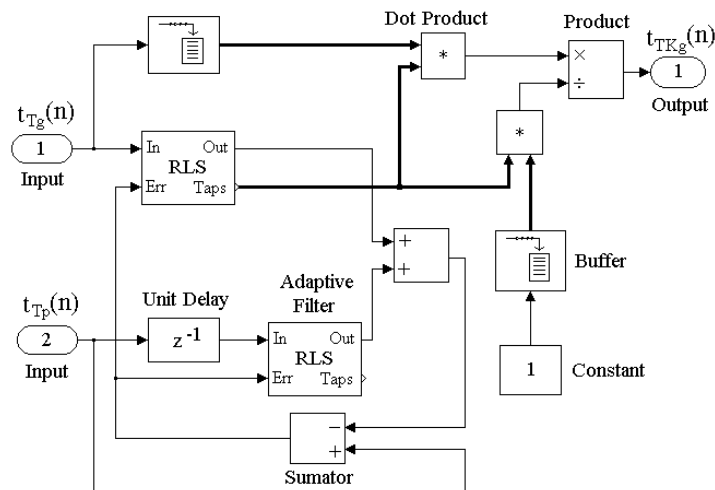


Fig. 12. Adaptive corrector in the two-sensor method – parameters updated after each sample.

The system with two sensors is shown in Fig.11 where: Tg , Kg - main sensor and main corrector, Tp , Kp - auxiliary sensor and auxiliary corrector, n - discrete time instant ($\tau = h \cdot n$). The role of the auxiliary corrector is to equalize the dynamic characteristic of the main sensor-main corrector path with the auxiliary sensor path. The auxiliary corrector parameters are determined on the basis of the auxiliary sensor parameters [15]. Identification of the auxiliary corrector parameters using the analog technique is difficult. Much easier implementation of the identification algorithm is possible in a digital or - more precisely - microprocessor system. The classical algorithms of adaptive signal processing, like LMS or RLS, can be used in their versions for discrete time dynamic models. The algorithm of the sensor parameters identification is derived in detail in [1,15] and the corrector block diagram implemented using MATLAB/Simulink v.5.2 is presented in Fig.12. Transfer of this diagram to newer versions of

MATLAB (v.7 when this work is published) does not involve problems. The input parameters of the corrector are: the order of digital adaptive filters, which are dynamic models of the main and auxiliary corrector, and the forgetting factor. The inputs of the corrector are the sensors signals while the reconstructed real temperature is the output. The block “Adaptive filter” that appears twice in Fig.12 is available in the *DSP Blockset* library in Simulink. The filter parameters are updated on the basis of the identification error, denoted “Error” in Fig.12, employing the RLS (Recursive Least Squares) algorithm. The next figure shows realizations of the adaptive filter (Fig.13a) and the RLS algorithm (Fig.13b) in Simulink.

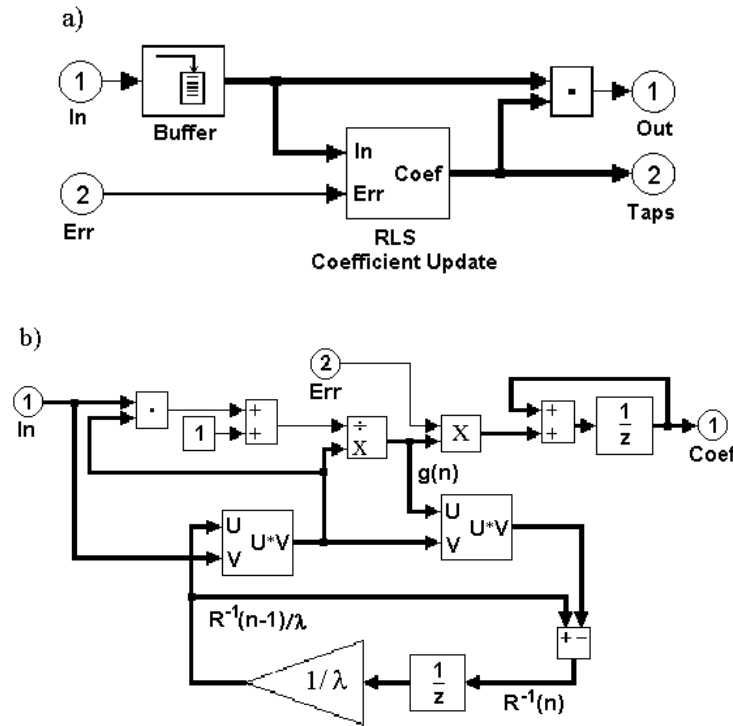


Fig. 13. (a) Adaptive filter, (b) RLS algorithm for updating the filter parameters

In measurement practice we often deal with nonstationary signals, i.e. signals whose autocorrelation function changes. For such signals we have give more weight to more recent samples than to old ones to ensure the convergence of the RLS algorithm. To achieve this, the algorithm uses the forgetting factor λ whose value should be chosen from the range (0.1). The algorithm with the forgetting factor matches the filter parameters to the variable dynamic properties of the sensor if it works e.g. in different heat transfer conditions or over a wide range of the temperature. To illustrate how the RLS version of the corrector works, we generated in MATLAB/Simulink waveforms from two nonlinear dynamic sensors. It was assumed that the dynamic parameters of the main and auxiliary sensor change linearly with temperature:

$$N_{T_g}(t_{T_g}) = N_{T_p} + bt_{T_g}, \quad (31a)$$

$$N_{T_p}(t_{T_p}) = cN_{T_p} + cbt_{T_p} \quad (31b)$$

and the dynamics is described by nonlinear first-order models. In Eqs. (31a) and (31b), N_{Tp} denotes the initial value of the dynamic parameter of the main sensor and c denotes the ratio of the dynamic parameters $N_{Tp}(t_{Tp})$ and $N_{Tg}(t_{Tg})$ of the auxiliary and main sensor respectively.

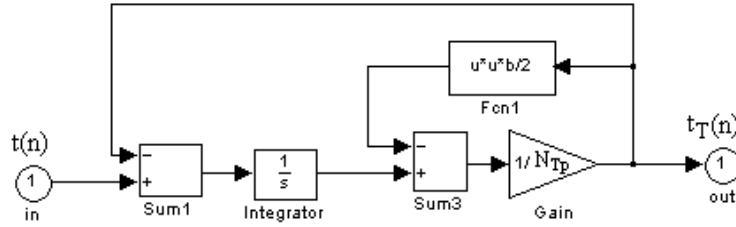


Fig. 14. Model of nonlinear sensor defined by equation (12) for $a=0$

The model of the nonlinear sensor is presented in Fig.14. The sensors were excited by a sum of three sine curves with the same amplitude and frequencies: 25 Hz, 50 Hz and 100 Hz. The amplitude of the input was normalized to the range $(0,1)$. It was also assumed that the random errors have a Gaussian distribution with a zero mean and the standard deviation $\delta = (1/3) \cdot 0.01$. This means that the probability of an error exceeding 1% of the maximum input is less than 1%. The sampling frequency $1/h$ was set to 8 kHz to comply with the standard frequency of the A/C converter on the test DSK board equipped with the TMS320C6713 signal processor from Texas Instruments. The 16-bit resolution of this converter was modelled using the quantizer block from Simulink.

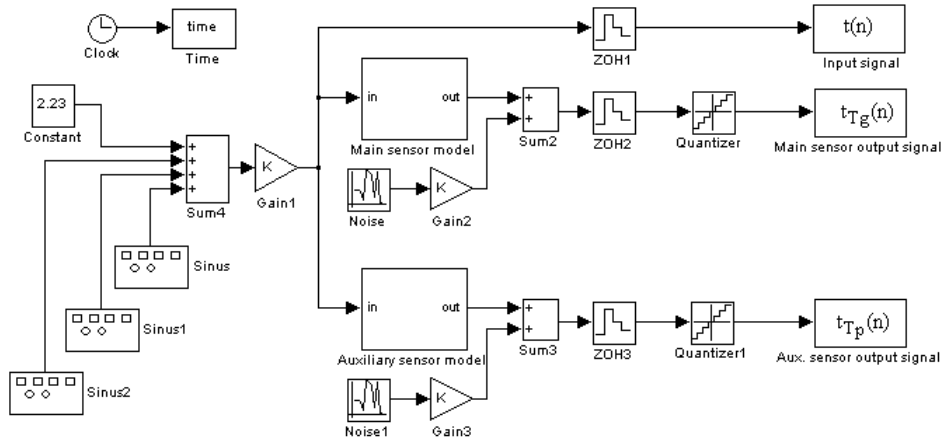


Fig. 15. Generation of signals processed by the corrector

We implemented the corrector shown in Fig.15 in MATLAB/Simulink v.7 and then we generated a machine code for the TMS signal processor using the *Embedded Target for TI C6000 DSP* tool. In the code we also implemented a 3rd-order digital Butterworth filter with the passband $f_{-3dB}/(1/2f_s) = 0.1$ to reduce the disturbances at the corrector input signal. It was also assumed that the order of the adaptive filters is 1 and the forgetting factor $\lambda = 0.98$. Examples of the signals from simulation of the system are shown in Fig.16.

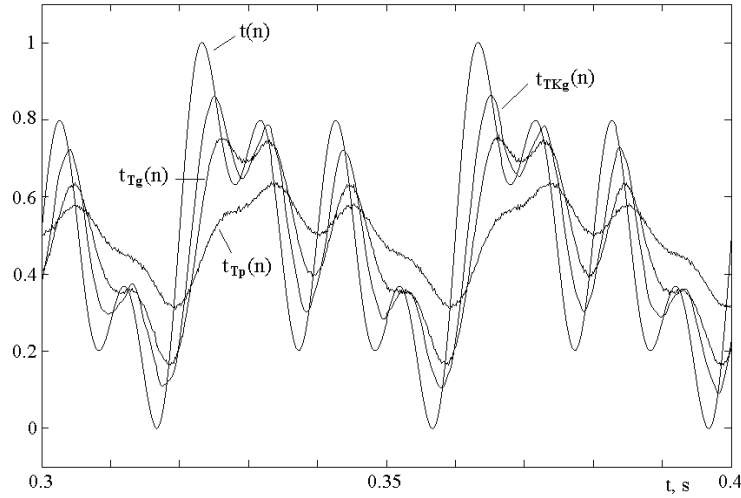


Fig. 16. Examples of output signals from the main sensor, auxiliary sensor and the main corrector.

They were obtained for the following parameters of the sensors: $N_{Tp} = 5\text{ms}$, $c=3$, $b/N_{Tp} = -0,5$. The ratio h/N_{Tp} satisfies condition (18). The waveforms in Fig.16 represent the „steady-state” because an initial period, when the corrector was tuning to the sensors’ dynamics, is omitted. We can see an increase of the amplitude of the corrector output signal $t_{TKg}(n)$ and a decrease of its phase shift with respect to the main sensor signal $t_{Tg}(n)$. However, the effect of the correction is limited due to the presence of the lowpass filter in the processing path, applying the linear corrector to the nonlinear sensors (models), errors of the identification method and numerical errors.

SUMMARY

The subject matter discussed in this work belongs to the dynamic metrology domain. The determination of the dynamic properties of the thermometer makes a significant reduction of the measurement error of the temperature either in steady state or arbitrarily varying in time possible. The accurate measurement of the temperature transforms into better control of a manufacturing process and better quality of products or rarer faults of power systems. The presented models and correction systems are in many ways universal so they can be applied, after modifications connected with specific operating conditions, in measurements of other physical quantities where the dynamics of sensors plays an important role. More information on the pulsatory method, mentioned in Fig.5 and omitted in this work, can be found e.g. in [1, 9].

NOTATION

T - temperature, K	τ - time, s
t - temperature, °C	N - time constant, s
Θ - temperature increment, K, °C	$N(t)$ - dynamic parameter, s
m - mass, kg	h - time increment, discretization step, s
c_p - specific heat, W·s/(kg·K)	d - diameter, mm
λ - thermal conductivity, W/(m·K)	ρ - density, kg/m ³
α - heat transfer coefficient, W/(m ² ·K)	F - area, m ²

Subscripts:
 T - thermometer,
 K - corrector,

TK - processing path thermometer-corrector,
 g - main,
 p - auxiliary, initial,
 m - maximum, steady.

REFERENCES

1. Minkina W., Gryś S.: *Dynamic properties correction of thermometric sensors - methods, circuits, algorithms*. Publishing house of Częstochowa University of Technology, Częstochowa 2004. (in Polish)
2. Minkina W., Gryś S.: *Dynamics of contact thermometric sensors with electric output and methods of its improving*. Symposium „Prospects and development forecast of automatics and metrology”, Szczecin-Niechorze 2005, pp. 43-58. (in Polish)
3. Żuchowski A.: *Identification of three-parameter dynamics' models on the basis of step response*. PAK 6/1997, pp. 170-172. (in Polish)
4. Żuchowski A.: *Determination of parameters of extended Strejc model by means of step response*. PAK, 7/2000, pp. 6-9. (in Polish)
5. Minkina W.: *Modelle für die Dynamik von Temperatursensoren*. Fachtagung „TEMPERATUR'89”, Suhl - Germany 1989, vol. 2, pp. 224-236. (in German)
6. Minkina W.: *Theoretical and experimental identification of the temperature sensor unit step response non-linearity during air temperature measurement*. Sensors & Actuators A:Physical, 1999, vol.A78, no.2-3, pp.81-87.
7. Benedict R.: *Fundamentals of Temperature, Pressure and Flow Measurements*. John Wiley&Sons Inc., New York-London-Sydney-Toronto 1969.
8. Puszer A.: *Calculation of step response specifications of shielded thermocouples*. PAK 7/8/1989, pp. 189-191. (in Polish)
9. Michalski L., Eckersdorf K., Kucharski J.: *Thermometry. Instruments and Methods*. Publishing house of Lodz University of Technology, Łódź 1998. (in Polish)
10. Żuchowski A.: *Recovering the input to the measurement system by means of the periodic use of several sensors*. 13th Symposium „Modelling and Simulation of Measuring Systems” (MiSSP), Kraków 2003, pp. 11-18. (in Polish)
11. Żuchowski A.: *Non-standard procedures for dynamics correction of measurement system*. Scientific Works of Silesian University of Technology, book series „Electrician”, no. 181, Gliwice 2002, pp. 209-218. (in Polish)
12. Šukšunov V.E.: *Correctors in transient temperature measurements*, Biblioteka po avtomatike, Energy, Moscow 1970. (in Russian)
13. Nabelec J.: *Blind correction of the I-order transducers*. 13th Symposium „Modelling and Simulation of Measuring Systems” (MiSSP), Kraków 2003, pp. 87-94. (in Polish)
14. Nalepa J.: *Effectiveness evaluation of the “blind” dynamical error correction - simulation of inertial first order measurement channel*. 11th Symposium „Modelling and Simulation of Measuring Systems” (MiSSP), Krynica Górská 2001, pp. 167-173. (in Polish)
15. Gryś S., Minkina W.: *Fast temperature determination using two thermometers with different dynamical properties*. Sensors & Actuators A: Physical, vol. A 100, no. 2-3, 2002, pp. 192-198.

DYNAMIKA STYKOWYCH CZUJNIKÓW TERMOMETRYCZNYCH O ELEKTRYCZNYM SYGNALE WYJŚCIOWYM I METODY JEJ POPRAWY

Streszczenie

W artykule przedstawiono wybrane zagadnienia dotyczące modelowania właściwości dynamicznych stykowych czujników termometrycznych oraz sposobami zmniejszania błędu dynamicznego występującego w pomiarze temperatury zmiennej w czasie oraz w trakcie ustalania się wskazań czujnika w pomiarze temperatury ustalonej. Ze względu na ograniczenia objętościowe powodujące konieczność pobieżnego przedstawienia pewnych zagadnień

niniejszy artykuł ma jedynie charakter poglądowy. Próbę szerszego opracowania tematycznego, zawierającego również wyniki prac własnych wraz z bogatą bibliografią podjęto w monografii autorów [1].